

## Structure–Activity Relationship Studies with Tetrahydroquinoline Analogs as EPAC Inhibitors

Yogesh A. Sonawane,<sup>†</sup> Yingmin Zhu,<sup>#</sup> Jered C. Garrison,<sup>§</sup> Edward L. Ezell,<sup>†</sup> Muhammad Zahid,<sup>||</sup> Xiaodong Cheng,<sup>#</sup> and Amarnath Natarajan<sup>\*,†,‡,§,⊥</sup>

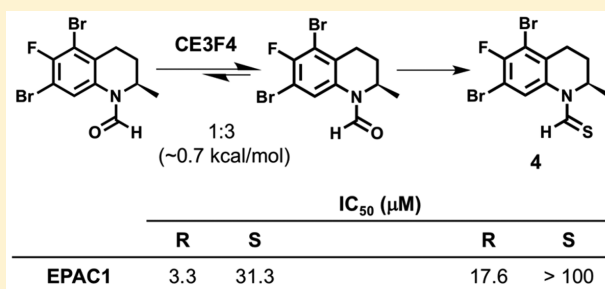
<sup>†</sup>Eppley Institute for Research in Cancer and Allied Diseases, <sup>‡</sup>Fred and Pamela Buffett Cancer Center, <sup>§</sup>Departments of Pharmaceutical Sciences, <sup>||</sup>Environmental, Agricultural and Occupational Health, and <sup>⊥</sup>Genetics Cell Biology and Anatomy, University of Nebraska Medical Center, Omaha, Nebraska 68022, United States

<sup>#</sup>Department of Integrative Biology and Pharmacology and Texas Therapeutics Institute, University of Texas Health Science Center, Houston, Texas 77030, United States

### Supporting Information

**ABSTRACT:** EPAC proteins are therapeutic targets for the potential treatment of cardiac hypertrophy and cancer metastasis. Several laboratories use a tetrahydroquinoline analog, CE3F4, to dissect the role of EPAC1 in various disease states. Here, we report SAR studies with tetrahydroquinoline analogs that explore various functional groups. The most potent EPAC inhibitor **12a** exists as a mixture of inseparable *E* (major) and *Z* (minor) rotamers. The rotation about the *N*-formyl group indeed impacts the activity against EPAC.

**KEYWORDS:** tetrahydroquinoline, exchange protein directly activated by cAMP, rotamer, dynamic NMR



Tetrahydroquinoline based natural products and analogs are known to have a wide range of biological activities including anticancer effects.<sup>1</sup> An *N*-formyl tetrahydroquinoline analog CE3F4 is used as an EPAC1-selective inhibitor.<sup>2–4</sup> EPAC proteins play a role in numerous cellular processes, which include insulin secretion, neurotransmitter release, integrin-mediated cell adhesion, cell survival, apoptosis, gene transcription, and chromosomal integrity.<sup>5–12</sup> EPAC1 is overexpressed in human pancreatic ductal adenocarcinoma (PDAC) samples, but the mechanism of this overexpression is unclear.<sup>11</sup> Migration and proliferation are key events in cancer progression,<sup>13</sup> and EPAC activation has been shown to regulate the proliferation and migration of prostate cancer cells.<sup>14</sup> As these cellular functions are crucial for tumor growth and metastasis, EPAC might represent an attractive therapeutic target in the treatment of cancers. Considering the important roles EPAC proteins play in physiological processes, the development of pharmacological probes that are isoform selective has attracted significant attention.<sup>15–17</sup> Here, we report the structure–activity relationship of tetrahydroquinoline (CE3F4) analogs, which includes the characterization of absolute configuration by X-ray crystallography. Our studies also revealed that the most potent EPAC1 inhibitor exists as a mixture of inseparable rotamers. Importantly, our studies reveal that the minor isomer is probably the major contributor of the EPAC1 activity.

In order to explore the role of the bromo substitutions ( $R_1$  and  $R_2$ ) on the phenyl ring, the stereochemistry (\*) at the C-2 position and the role of the *N*-formyl group ( $R_3$ ) on CE3F4, we

synthesized a focused library of tetrahydroquinoline analogs (Figure 1). The key steps in the synthesis are (i) reduction of

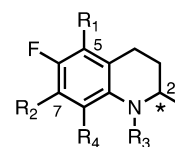


**Figure 1.** Positions on the tetrahydroquinoline explored in the structure–activity relationship studies.

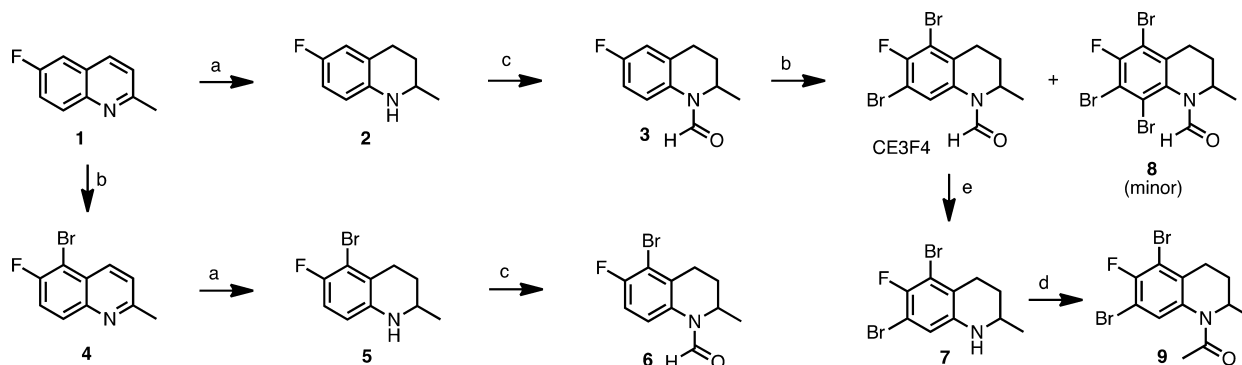
the commercially available 6-fluoro-2-methylquinoline **1** to yield the racemic tetrahydroquinoline core, (ii) bromination of the aryl ring, (iii) resolution using a chiral auxiliary, and (iv) formylation of the tetrahydroquinoline nitrogen.

To explore the role of the bromine atoms on the phenyl ring we generated analogs **3**, **6**, CE3F4, and **8**. Unlike CE3F4, which is a 5,7-dibromo compound analog, **3** does not contain bromine atoms, analog **6** is a 5-bromo analog, and analog **8** is a tribromo compound. A Pt/C-catalyzed reduction of 6-fluoro-2-methylquinoline **1** yielded a 6-fluoro-2-methyltetrahydroquinoline core.<sup>18</sup> Formylation of tetrahydroquinoline **2** was accomplished using acetic anhydride and formic acid to generate analog **3** (Scheme 1).

**Received:** August 29, 2017

**Accepted:** October 2, 2017

**Published:** October 2, 2017

Scheme 1. Synthesis of Tetrahydroquinoline Analogs<sup>a</sup>

<sup>a</sup>Reagents and conditions: (a) 5% Pt/C, AcOH, H<sub>2</sub>, rt, 16 h; (b) AlCl<sub>3</sub>, Br<sub>2</sub>, 1,2-dichloroethane, 60 °C, 3 h; (c) acetic anhydride, formic acid, 0–50 °C, 6 h; (d) acetyl chloride, pyridine, DCM, 0 °C, 2 h; (e) 10% HCl, EtOH, reflux, 4 h.

Complexation with aluminum chloride (AlCl<sub>3</sub>) deactivates the pyridine ring and increases the electron density at the 5- and 8-positions. Consequently, electrophilic aromatic substitution of 6-halogenated quinolines or tetrahydroquinolines results in 5-substituted, 8-substituted, or 5,8-substituted analogs. AlCl<sub>3</sub>/Br<sub>2</sub>-mediated bromination of **1** resulted in 5-bromo-6-fluoro-2-methylquinoline **4** as the major product. A Pt/C-catalyzed reduction followed by formylation using acetic anhydride and formic acid yielded the monobromo-*N*-formyl tetrahydroquinoline **6**. Bromination using AlCl<sub>3</sub>/Br<sub>2</sub> of analog **3** yielded CE3F4. Careful chromatography resulted in the isolation of **8**, the tribromo compound, as a minor product.

Analogs **9** and **7** were synthesized to assess the role of the formyl group in CE3F4. The acetyl variant **9** was generated in two steps. The formyl group was removed from CE3F4 under acidic conditions to generate analog **7**, which was acetylated to generate **9**.

Courilleau et al. reported an SAR of tetrahydroquinoline analogs which included compounds **6**, **7**, and **9** in Table 1.<sup>3</sup> The

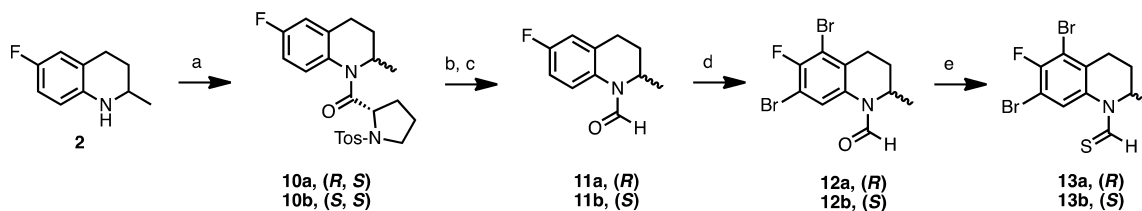
present study expands on this SAR and includes additional analogs and characterization of all compounds evaluated. The tetrahydroquinoline analogs were analyzed for their ability to inhibit EPAC1 activation. EPAC1 was stimulated in the presence of 10 and 50 μM of the tetrahydroquinoline analogs. The activity of the inhibitors was screened using a BODIPY-GDP-based guanine nucleotide exchange factor (GEF) activity assay of Rap1 as described previously.<sup>19</sup> The 5-bromo-substituted analog **6** was ~3-fold more potent than analog **3** that does not have the Br atom at the 5 position. The 5,7-dibromo analog CE3F4 was ~4-fold more potent than the monobromo analog **6**. Interestingly, adding another bromine atom at the C-8 position resulted in a ~2.5-fold loss of activity. A comparison of CE3F4, **9**, and **7** shows that replacing the formyl group with an acetyl in **9** or removal of the formyl group in **7** resulted in loss of activity. We also evaluated the *R* and *S* isomers of **3**, **6**, and **7** to determine the effect of the stereocenter on EPAC activity (Table S1). The data shows that the presence of the formyl group makes the *R* analogs more potent than the *S* analogs. For example, 6*R* is ~3-fold more potent than 6*S*. On the other hand, in the absence of the formyl group the *S* analog is more potent than the *R* analog (7*S* analog is ~7-fold more potent than 7*R*). Together, these demonstrate that 1-formyl, 6-fluoro, and 5,7-dibromo substitution on the tetrahydroquinoline is optimal for the inhibition of EPAC1 activity (Table 1).

Coupling of 6-fluoro-2-methyl-1,2,3,4-tetrahydroquinoline **2** with tosyl-*S*-prolinoyl chloride resulted in diastereoisomers **10a** and **10b** (Scheme 2).<sup>20</sup> The diastereomeric mixture was column separable and the individual isomers were separated using an isocratic 9:1, dichloromethane and ethyl acetate mobile system. The absolute configuration of the diastereoisomers was determined by X-ray crystallography analyses (Figure S1).

Table 1. Evaluation of Tetrahydroquinoline Analogs

no.	R <sub>1</sub>	R <sub>2</sub>	R <sub>3</sub>	R <sub>4</sub>	% EPAC inhibition	
					low <sup>a</sup>	high <sup>b</sup>
<b>3</b>	H	H	CHO	H	5.3	5.0
<b>6</b>	Br	H	CHO	H	15.8	42.0
CE3F4	Br	Br	CHO	H	58.1	88.3
<b>7</b>	Br	Br	H	H	40.8	74.1
<b>8</b>	Br	Br	CHO	Br	23.6	46.0
<b>9</b>	Br	Br	COCH <sub>3</sub>	H	8.7	26.2

<sup>a</sup>10 μM. <sup>b</sup>50 μM.

Scheme 2. Synthesis of Tetrahydroquinoline Enantiomers<sup>a</sup>

<sup>a</sup>Reagents and conditions: (a) tosyl-*S*-prolinoyl chloride, DIPEA, DCM, 5–10 °C, 30 min. reflux; (b) NaOEt, EtOH, reflux, 6 h; (c) acetic anhydride, formic acid, 0–50 °C, 6 h; (d) AlCl<sub>3</sub>, Br<sub>2</sub>, 1,2-dichloroethane, 60 °C, 3 h; (e) Lawesson's reagent, toluene, 100 °C, 6 h.

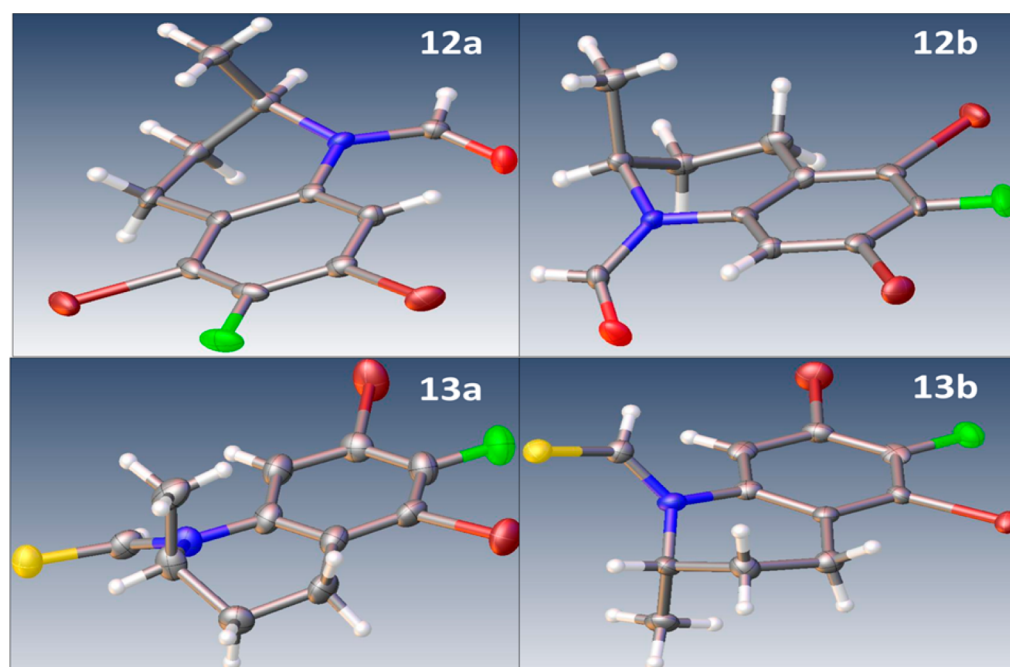


Figure 2. X-ray crystal structures of 12a, 12b, 13a, and 13b.

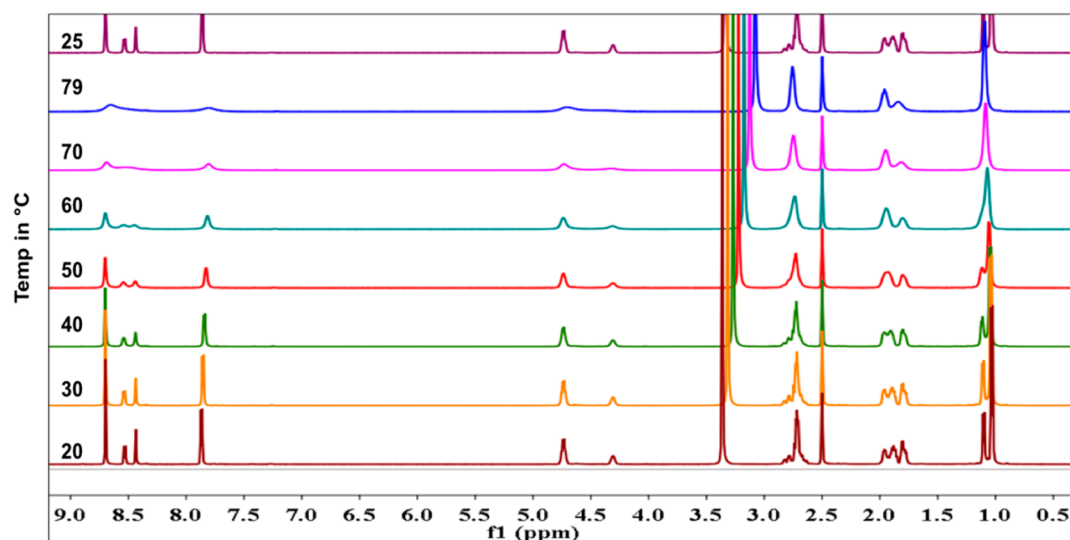


Figure 3. Variable-temperature  $^1\text{H}$  NMR spectra of 12a in  $\text{DMSO}-d_6$  from 20 to 79  $^\circ\text{C}$  demonstrating the presence of rotamers.

Bromination of the individual isomers resulted in 12a and 12b (*R*- and *S*-CE3F4). We also generated the corresponding thioformyl isomers 13a and 13b using Lawesson's reagent. The absolute configurations of 12a, 12b, 13a, and 13b were established by X-ray crystallography (Figure 2).

$^1\text{H}$  NMR of 12a and 12b revealed that they exist as a mixture of two rotamers in a 3:1 ratio. It is well-known that *N*-formyl compounds exist in a solution as interconverting rotamers. Rotation about the *N*-formyl (*N*-CO) bond has been of great interest to organic chemists.<sup>21–23</sup> NMR studies have been used to estimate the energy barrier for the rotamer interconversion<sup>24</sup> in compounds such as *N*-formyl-1-bromo-4-hydroxy-3-methoxymorphinan-6-one, the key intermediate in opiate synthesis.<sup>25</sup> We conducted a temperature-dependent NMR study to confirm that 12a indeed exists as a pair of interconverting rotamers in solution.

We observed peak broadening for a subset of peaks at higher temperatures, which is due to the dynamic exchange between the two rotamers (Figure 3 and Figure S2).

A complete coalescence was observed for all signals at 79  $^\circ\text{C}$ . The reversibility of these changes was verified when the experimental temperature was returned to 25  $^\circ\text{C}$ . We used the data obtained from the variable temperature NMR studies to calculate the energy barrier. The energy barrier (avg) for the major to minor is 16.6 kcal/mol, while the energy barrier (avg) for the minor to major rotamer is 15.9 kcal/mol (Table S2). The major rotamer (*E*) is  $\sim 0.7$  kcal/mol more stable than the minor rotamer (*Z*).

We conducted NOESY experiments with mixing times of 50, 200, and 400 ms to assign the signals for the two rotamers. The peak volumes measured by the NOE experiments correlated with the distance between the formyl hydrogen atom and the hydrogen atom at the C-2 position (Figure 4 and Figure S3).

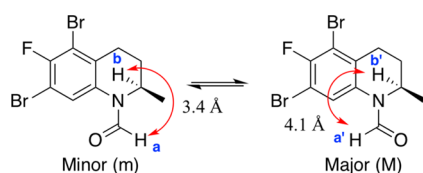


**Figure 4.** Major and minor rotamers determined based on NOESY spectra.

To determine the rate of interconversion we dissolved the crystals in DMSO- $d_6$  for a quick  $^1\text{H}$  NMR. Remarkably, we observed the rotamers in a  $\sim$ 3:1 ratio, indicating the rapid equilibration in a solution.

A comparison of the NMR and crystallography study resulted in a rather puzzling conundrum wherein only the minor rotamer crystallized. Crystallography data suggests that the packing interactions are probably better in the minor rotamer. Thioamide is a well-known isosteric replacement of amides. The larger charge transfer from *N* to *S* in thioamides results in increased *C*-*N* rotational barrier by  $\sim$ 5 kcal/mol when compared to the corresponding amides.<sup>26</sup> Based on this, we speculated that a thioformyl analog (**13a** in Scheme 2) will adopt the *E* geometry, consistent with the major rotamer of **12a**. NMR studies revealed that analog **13a** is a single rotamer (Figure S4). NOESY studies revealed that the *N*-thioformyl group indeed adopts the *E* conformation, which is consistent with what was observed by X-ray crystallography (Figure 2, **13a** and **13b**).

We also explored the solvent effect on the rotamer ratio ( $\text{C}_6\text{D}_6$ ,  $\text{CDCl}_3$ ,  $\text{CD}_2\text{Cl}_2$ ,  $\text{CD}_3\text{COCD}_3$ , and  $\text{CD}_3\text{CN}$ ) and found that the major isomer was slightly more favored in the nonpolar solvents (Figure S5). Since **12a** and **12b** will be used for biological studies, we wondered if the rotamer ratio will be influenced by the presence of water. To test this, we conducted  $^1\text{H}$  NMR studies with increasing ratios of  $\text{D}_2\text{O}/\text{DMSO-}d_6$ . The rotamer ratio of 3:1 was stable even at 40%  $\text{D}_2\text{O}$  (Figure S6), indicating that the rotamers exist in aqueous solutions.

We next explored the effect of the stereochemistry at the *C*-2 position with analogs **12a** and **12b** on EPAC1 activity and selectivity. The *R*-isomer **12a** was  $\sim$ 10-fold more potent against EPAC1 than the *S*-isomer **12b**. The *R*-isomer was  $\sim$ 7-fold selective for EPAC1 over EPAC2; interestingly, the selectivity was reversed with the *S*-isomer (Table 2). This demonstrates

**Table 2.** Evaluation of **12a**, **12b**, **13a**, and **13b**

	$\text{IC}_{50}$ ( $\mu\text{M}$ )	
	EPAC1	EPAC2
<b>12a</b>	$3.3 \pm 0.4$	$22.3 \pm 2.1$
<b>12b</b>	$31.3 \pm 9.2$	$17.1 \pm 3.5$
<b>13a</b>	$17.6 \pm 6.5$	N/D
<b>13b</b>	>100	N/D

that the enantiomers engage EPAC1 and EPAC2 differently, and the cocrystal structure of EPAC1 and EPAC2 with the enantiomers will reveal the differences in their binding modes.

Analog **13a** is  $\sim$ 5-fold less active than **12a**. This is because **12a** exists as a mixture of rotamers while **13a** does not. Compound **13a** adopts the conformation that corresponds to the major rotamer conformation of **12a**. The loss of activity associated with **13a** suggests that the minor rotamer conformation of **12a** is the major contributor to the EPAC1

activity. This is partially supported by the lower activity observed with analog **8** (Table 1) that could potentially restrict access to the minor conformation due to steric hindrance. The present study does not address if demethylation (2-position) of analog **12** will eliminate the rotamers; i.e., the formyl group on such an analog will adopt the conformation that corresponds to the major rotamer in **12**. It is also possible that the rotamer distribution is dictated by hypothetical hydrogen bonds between the formyl oxygen atom and the hydrogen atoms at the 2-position methyl group and/or the 8-position on the phenyl ring.

In conclusion, we report a route (24% overall yield) for gram-scale synthesis of the EPAC1 inhibitor **12a** with low  $\mu\text{M}$  potency. The structure–activity relationship study demonstrates that the two bromine atoms and the formyl group are critical for activity. Moreover, the importance of the stereochemistry at the *C*-2 position on activity and selectivity of **12a** was demonstrated. Herein, we provide extensive chemical and structural characterization of **12a**. NMR studies revealed that **12a** exists as a mixture of inseparable rotamers in a 3:1 ratio. The minor **12a** rotamer crystallized, indicating better packing interaction, and when the crystals were dissolved they rapidly equilibrated to the 3:1 ratio. Studies with the thio analog **13a** revealed that it exists as a single compound that corresponds to the major rotamer in **12a**. Importantly, EPAC activity studies with **12a**, **12b**, **13a**, and **13b** indicate that the minor rotamer could be the major contributor to the EPAC1 activity.

## ■ ASSOCIATED CONTENT

### Supporting Information

The Supporting Information is available free of charge on the ACS Publications website at DOI: 10.1021/acsmchemlett.7b00358.

- Experimental procedures, characterization data, supporting figures, crystallographic details, theoretical calculations, and compound spectral data (PDF)
- X-ray crystallographic data for **10a** (*R,S*) (CIF)
- X-ray crystallographic data for **10b** (*S,S*) (CIF)
- X-ray crystallographic data for **12a** (CIF)
- X-ray crystallographic data for **12b** (CIF)
- X-ray crystallographic data for **13a** (CIF)
- X-ray crystallographic data for **13b** (CIF)

## ■ AUTHOR INFORMATION

### Corresponding Author

\*Tel: (402) 559-3793. Fax: (402) 559-8270. E-mail: anatarajan@unmc.edu.

### ORCID

Yogesh A. Sonawane: 0000-0002-6799-7525

Jered C. Garrison: 0000-0002-8376-9821

Amarnath Natarajan: 0000-0001-5067-0203

### Funding

A.N. is supported by the Eppley Pilot Grant, Fred and Pamela Buffett Cancer Center Support Grant from NIH (P30CA036727). X.C. is supported by funding from NIH (R01GM066170 and R35GM122536).

### Notes

The authors declare no competing financial interest.

## ACKNOWLEDGMENTS

The authors thank the lab members for their valuable suggestions and critiques.

## ABBREVIATIONS

EPAC, exchange protein activated by cAMP; PDAC, pancreatic ductal adenocarcinoma; BODIPY-GDP, guanosine diphosphate–boron–dipyromethene; GEF, guanine nucleotide exchange factor; SAR, structure–activity relationship; NMR, nuclear magnetic resonance; TLC, thin-layer chromatography; HPLC, high-performance liquid chromatography; MS, mass spectrometry; DMSO, dimethyl sulfoxide; NOESY, nuclear Overhauser effect

## REFERENCES

- (1) Sridharan, V.; Suryavanshi, P. A.; Menendez, J. C. Advances in the chemistry of tetrahydroquinolines. *Chem. Rev.* **2011**, *111*, 7157–259.
- (2) Courilleau, D.; Bissierier, M.; Jullian, J.-C.; Lucas, A.; Bouyssou, P.; Fischmeister, R.; Blondeau, J.-P.; Lezoualc'h, F. Identification of a tetrahydroquinoline analog as a pharmacological inhibitor of the cAMP-binding protein Epac. *J. Biol. Chem.* **2012**, *287*, 44192–44202.
- (3) Courilleau, D.; Bouyssou, P.; Fischmeister, R.; Lezoualc'h, F.; Blondeau, J.-P. The (R)-enantiomer of CE3F4 is a preferential inhibitor of human exchange protein directly activated by cyclic AMP isoform 1 (Epac1). *Biochem. Biophys. Res. Commun.* **2013**, *440*, 443–448.
- (4) Lezoualc'h, F.; Fischmeister, R.; Bissierier, M.; Bouyssou, P.; Blondeau, J. P.; Courilleau, D. Tetrahydroquinoline Derivatives and Their Use as EPAC Inhibitors. US 20150252002A1, 2015.
- (5) Tsalkova, T.; Mei, F. C.; Cheng, X. A fluorescence-based high-throughput assay for the discovery of exchange protein directly activated by cyclic AMP (EPAC) antagonists. *PLoS One* **2012**, *7*, e30441.
- (6) Cheng, X.; Ji, Z.; Tsalkova, T.; Mei, F.; Epac, P. K. A. A Tale of Two Intracellular cAMP Receptors. *Acta Biochim. Biophys. Sin.* **2008**, *40*, 651–662.
- (7) Grandoch, M.; Roscioni, S. S.; Schmidt, M. The role of Epac proteins, novel cAMP mediators, in the regulation of immune, lung and neuronal function. *Br. J. Pharmacol.* **2010**, *159*, 265–284.
- (8) Schmidt, M.; Dekker, F. J.; Maarsingh, H. Exchange protein directly activated by cAMP (epac): a multidomain cAMP mediator in the regulation of diverse biological functions. *Pharmacol. Rev.* **2013**, *65*, 670–709.
- (9) Laurent, A.-C.; Bissierier, M.; Lucas, A.; Tortosa, F.; Roumieux, M.; De Régibus, A.; Swiader, A.; Sainte-Marie, Y.; Heymes, C.; Vindis, C. Exchange protein directly activated by cAMP 1 promotes autophagy during cardiomyocyte hypertrophy. *Cardiovasc. Res.* **2015**, *105*, 55–64.
- (10) Almahariq, M.; Tsalkova, T.; Mei, F. C.; Chen, H.; Zhou, J.; Sastry, S. K.; Schwede, F.; Cheng, X. A novel EPAC-specific inhibitor suppresses pancreatic cancer cell migration and invasion. *Mol. Pharmacol.* **2013**, *83*, 122–128.
- (11) Lorenz, R.; Aleksic, T.; Wagner, M.; Adler, G.; Weber, C. K. The cAMP/Epac1/Rap1 pathway in pancreatic carcinoma. *Pancreas* **2008**, *37*, 102–103.
- (12) Chen, H.; Wild, C.; Zhou, X.; Ye, N.; Cheng, X.; Zhou, J. Recent Advances in the Discovery of Small Molecules Targeting Exchange Proteins Directly Activated by cAMP (EPAC). *J. Med. Chem.* **2014**, *57*, 3651–3665.
- (13) Abate-Shen, C.; Shen, M. M. Molecular genetics of prostate cancer. *Genes Dev.* **2000**, *14*, 2410–2434.
- (14) Grandoch, M.; Rose, A.; Ter Braak, M.; Jendrossek, V.; Rübber, H.; Fischer, J.; Schmidt, M.; Weber, A. Epac inhibits migration and proliferation of human prostate carcinoma cells. *Br. J. Cancer* **2009**, *101*, 2038.
- (15) Kumar, N.; Gupta, S.; Dabral, S.; Singh, S.; Sehrawat, S. Role of exchange protein directly activated by cAMP (EPAC1) in breast cancer cell migration and apoptosis. *Mol. Cell. Biochem.* **2017**, *430*, 115–125.
- (16) Holz, G. G.; Chepurny, O. G.; Schwede, F. Epac-selective cAMP analogs: new tools with which to evaluate the signal transduction properties of cAMP-regulated guanine nucleotide exchange factors. *Cell. Signalling* **2008**, *20*, 10–20.
- (17) Tsalkova, T.; Mei, F. C.; Li, S.; Chepurny, O. G.; Leech, C. A.; Liu, T.; Holz, G. G.; Woods, V. L.; Cheng, X. Isoform-specific antagonists of exchange proteins directly activated by cAMP. *Proc. Natl. Acad. Sci. U. S. A.* **2012**, *109*, 18613–18618.
- (18) Bouyssou, P.; Le Goff, C.; Chenault, J. Synthesis of 7-and 5, 7-substituted-6-fluoro-2-methyl-1, 2, 3, 4-tetrahydroquinolines: Convenient precursors of quinolone antibacterial agents. *J. Heterocycl. Chem.* **1992**, *29*, 895–898.
- (19) Zhu, Y.; Chen, H.; Boulton, S.; Mei, F.; Ye, N.; Melacini, G.; Zhou, J.; Cheng, X. Biochemical and pharmacological characterizations of ESI-09 based EPAC inhibitors: Defining the ESI-09 “therapeutic window. *Sci. Rep.* **2015**, *5*, 9344.
- (20) Gruzdev, D.; Vakarov, S.; Levit, G.; Krasnov, V. N-Tosyl-(S)-Prolyl Chloride in Kinetic Resolution of Racemic Heterocyclic Amines. *Chem. Heterocycl. Compd.* **2014**, *49*, 1795.
- (21) Wiberg, K. B.; Rush, D. J. Solvent effects on the thioamide rotational barrier: An experimental and theoretical study. *J. Am. Chem. Soc.* **2001**, *123*, 2038–2046.
- (22) Wiberg, K. B.; Breneman, C. M. Resonance interactions in acyclic systems. 3. Formamide internal rotation revisited. Charge and energy redistribution along the CN bond rotational pathway. *J. Am. Chem. Soc.* **1992**, *114*, 831–840.
- (23) Rablen, P. R.; Miller, D. A.; Bullock, V. R.; Hutchinson, P. H.; Gorman, J. A. Solvent Effects on the Barrier to C–N Bond Rotation in N, N-Dimethylaminoacrylonitrile. *J. Am. Chem. Soc.* **1999**, *121*, 218–226.
- (24) Hu, D. X.; Grice, P.; Ley, S. V. Rotamers or diastereomers? An overlooked NMR solution. *J. Org. Chem.* **2012**, *77*, 5198–5202.
- (25) Sulima, A.; Cheng, K.; Jacobson, A. E.; Rice, K. C.; Gawrisch, K.; Lee, Y.-S. Z. and E rotamers of N-formyl-1-bromo-4-hydroxy-3-methoxymorphinan-6-one and their interconversion as studied by (1)H/(13)C NMR spectroscopy and quantum chemical calculations. *Magn. Reson. Chem.* **2013**, *51*, 82–88.
- (26) Olszewska, T.; Pyszno, A.; Milewska, M. J.; Gdaniec, M.; Poloński, T. Thioamides and selenoamides with chirality solely due to hindered rotation about the C–N bond: enantioselective complexation with optically active hosts. *Tetrahedron: Asymmetry* **2005**, *16*, 3711–3717.